Accepted Manuscript

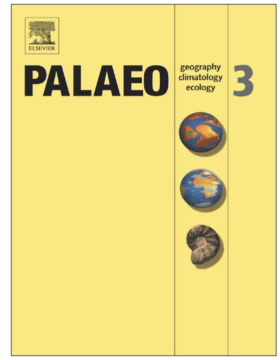

Disentangling dust and sand deposition using a peat record in CE Europe (northern Romania): A multiproxy approach

Andrei Marian Panait, Simon Mark Hutchinson, Andrei-Cosmin Diaconu, Ioan Tanţău, Angelica Feurdean

PII: S0031-0182(18)30914-3
DOI: https://doi.org/10.1016/j.palaeo.2019.109257
Article Number: 109257
Reference: PALAEO 109257

To appear in: *Palaeogeography, Palaeoclimatology, Palaeoecology*

Received date: 4 November 2018
Revised date: 24 May 2019
Accepted date: 27 June 2019

Please cite this article as: A.M. Panait, S.M. Hutchinson, A.-C. Diaconu, et al., Disentangling dust and sand deposition using a peat record in CE Europe (northern Romania): A multiproxy approach, Palaeogeography, Palaeoclimatology, Palaeoecology, https://doi.org/10.1016/j.palaeo.2019.109257

This is a PDF file of an unedited manuscript that has been accepted for publication. As a service to our customers we are providing this early version of the manuscript. The manuscript will undergo copyediting, typesetting, and review of the resulting proof before it is published in its final form. Please note that during the production process errors may be discovered which could affect the content, and all legal disclaimers that apply to the journal pertain.

ACCEPTED MANUSCRIPT

Disentangling dust and sand deposition using a peat record in CE Europe (northern Romania): a multiproxy approach

Andrei Marian Panait [1*], Simon Mark Hutchinson [2], Andrei-Cosmin Diaconu [1], Ioan Tanţău [1], Angelica Feurdean [1, 3]

[1] Department of Geology, Babes-Bolyai University, 400084 Cluj-Napoca, Romania. pnt_andrei@yahoo.com; pnt_andrei@yahoo.com; ioan.tantau@ubbcluj.ro

[2] School of Environment and Life Sciences, University of Salford, Salford M5 4WT, UK. s.m.hutchinson@salford.ac.uk

[3] Senckenberg Biodiversity and Climate Research Centre, Senckenberganlange 25, D-60325 Frankfurt am Main, Germany. angelica.feurdean@senckenberg.de

***Corresponding author**. Andrei-Marian Panait; Department of Geology, Babeş-Bolyai University, Cluj-Napoca, Romania, Kogălniceanu 1, 40008. pnt_andrei@yahoo.com

Abstract

Aeolian sediments play an important role in the global climatic system and occur in the atmosphere due to soil and bedrock erosion. Here, we applied three different methods: geochemical (XRF), manual and laser-based particle size analysis to an ombrotrophic peat profile in the Carpathian Mountains to determine changes in aeolian deposition and wind / storm activity over the last 7800 years. The results show four changes in aeolian fluxes (dust and sand) over time: 7800-4150 cal. yr BP – generally low dust fluxes with a periodic intensification of sand fluxes; 4150-2300 cal.

ACCEPTED MANUSCRIPT

yr BP – intense deposition of both dust and sand; 2300-150 cal. yr BP – fluctuating dust and sand fluxes; the last 200 years – the highest amplitude of both sand and dust fluxes. This study found that patterns in aeolian fluxes were primarily influenced by climate, but with anthropogenic drivers, such as disturbance by fire, becoming more important in recent times. We also found a good agreement with other studies of dust fluxes for the earlier part of this record before 3500 cal. yr BP, but an increasing divergence over the last 3500 years. In terms of a methodological approach, we suggest that the three approaches each have both advantages and disadvantages; though overall laser-based particle size dust and sand reconstruction appears to best capture the most complex changes in both aeolian deposition rates and sources.

Keywords: aeolian particles, geochemistry, particle size analysis, manually counting of sand particles, particulate mineralogy.

1. Introduction

Mineral dust plays an important role in climate systems influencing the radiative properties of the atmosphere by reflecting and absorbing solar radiation, and, indirectly, by affecting cloud formation and thereby precipitation patterns (Sassen et al., 2003). Mineral dusts also play a role in atmospheric chemistry and fertilisation processes acting as a source of nutrients to biological systems (Kohfeld and Harrison, 2001). Fine particles in the atmosphere can also impact human health (Goudie and Middleton, 2006; Field et al., 2010).

Atmospheric dust (<63 μm) originates primarily from arid and semi-arid regions where vegetation cover is sparse exposing source areas and where the velocity of winds permits the entrainment of silt-sized material into the atmosphere (Middleton

ACCEPTED MANUSCRIPT

and Goudie, 2001; Grousset and Biscaye, 2005). Local factors i.e., agriculture and deforestation which expose surfaces and affect wind flow can also influence dust composition and deposition (Tegen et al., 2004). Lawrence and Neff (2009) showed that dust deposition is primary influenced by dust concentrations in the atmosphere, precipitation and vegetation cover. Therefore, fluctuations in dust loading may be indicative of both regional drying and disturbance as well as long-distance wind transport (Le Roux et al., 2012). Conversely, sand, due to its larger diameter (63-2000 μm), cannot be transported by wind over long distances and it is therefore likely to originate from local sources.

The chemical composition of dust in the atmosphere will not remain constant over time, but reflect the mineralogy of the particles in suspension and so will change as source areas shift (Kylander et al., 2016). However, it is believed that dust mainly reflects the composition of the earth's crust (Shotyk et al. 2002). However, after deposition, for example in peat bogs, dust geochemistry can change and consequently may not readily reflect its original composition (Shotyk et al. 2002). Nevertheless, it is known that some geochemical elements are conservative (e.g. Ti, Zr, rare earth elements) and consequently can faithfully indicate changes in dust deposition (Shotyk et al. 2002). Therefore, the presence of fine mineral particles in ombrogenous peatlands can provide insights into dust transport, deposition and even provenance.

During the Quaternary, global dust fluxes have shown a strong variability with marked increases during the glacial periods (Mahowald et al. 1999) as reflected by extensive loess deposits and the dust found in ice cores and ocean sediments (Muhs and Bettis 2000; Shichang et al. 2001; Pichevin et al. 2005). Within the current interglacial period, a link between climate, anthropogenic impact and atmospheric

ACCEPTED MANUSCRIPT

dust and sand deposition can be determined based on the aeolian particles held in ombrogenous mires. Most studies concerning European Holocene intracontinental atmospheric dust and sand deposition are based on lake (Jiménez-Espejo et al, 2014; Dreibrodt and Wiethold et al, 2014; Kalińska-Nartiša et al. 2015; Woronko and Bujak, 2018) and peat archives from NW Europe (e.g. Shotik et al., 2002; Björck and Clemmensen, 2004; de Jong et al 2006, 2007; Gabrielli et al., 2010; Allan et al., 2013; Kylander et al., 2013, 2016) or from other parts of the world (e.g. Sapkota, 2006; Marx et al., 2011; Lambert et al., 2012). However, records of past aeolian deposition in peat archives from Central and Eastern Europe (CEE) are scarce (De Vleeschouwer et al., 2009; Longman et al., 2017) even though peat archives in this region are abundant. Peat archives in this part of Europe have predominantly been investigated using pollen analysis (Feurdean, 2010; Tanţău et al., 2011; 2014a,b; Fărcaş et al., 2013; Feurdean et al., 2016). However, some recent studies have focused on hydro-climate variability based on testate amoeba and $\delta^{13}C$ isotopic composition (Schnitchen et al., 2006, Cristea et al., 2014; Feurdean et al., 2015; Diaconu et al., 2017) and geochemistry (Haliuc et al., 2016; Longman et al., 2017, 2019).

Here we use a multi-proxy approach (loss on ignition, instrument-based and manual estimates of grain size and type, and peat geochemistry) on a peat sequence from a mountain ombrogenous bog (Tăul Muced) located in the north of the Eastern Carpathians, Romania to explore changes in aeolian dust and sand deposition over the last 7800 years. The specific aims are to:

1. Determine changes in atmospheric dust and sand deposition and assess their association with climate conditions and land use changes.

2. Investigate the regional-scale relationship between records across the wider region.

ACCEPTED MANUSCRIPT

This study is one of the first concerning mid-late Holocene sand and dust influxes in CEE and the first that explores local minerogenic influxes. Furthermore, it brings a new approach using established methods in combination to the study of aeolian inputs in ombrogenous peat bogs.

2. Study area

Tăul Muced peat bog (47°34’ 26’’ N, 24° 32’42’’ E; 1360 m a.s.l.; 2 ha) is located in northern Romania in the Eastern Carpathians in the Rodna Mountains (Fig. 1A). It lies within the Rodna National Park and Biosphere Reserve. The site is an ombrotrophic raised bog presently dominated by *Sphagnum russowii* and *S. magellanicum* (Feurdean et al. 2015); the topography immediately surrounding the site is level precluding the input of surface runoff. The vegetation around the site consists of a dense forest of Norway spruce (*Picea abies*) (Feurdean et al. 2015). The mire’s initial development (500 to 459 cm depth) was characterised by an abundance of Cyperaceae, followed by the dominance of *Sphagnum* species, which indicate the peat’s ombrotrophy (Galka et al. 2016).

The local geology comprises a basement of Precambrian crystalline rocks: mica schist, quartzite, marble, dolomitic marble (Bercia et al., 1976; Sahy et al., 2008; Tămaş et al., 2011; Fig. 1B). Sedimentary deposits locally are Eocene and Oligocene and are mainly sandstones, limestones and black shales. Conglomerate and black shales are found closest to the site and, as both are susceptible to erosion, could be the main source of local aeolian inputs. Crystalline rocks and limestones are located further away and their influence on the peatbog is probably less significant. The landscape of the peatbog is located on a relatively flat landscape; therefore, surface

ACCEPTED MANUSCRIPT

runoff is almost non-existent/

Climatically, the study area has a moderate temperate continental climate with Atlantic and Baltic influences. Mean annual temperature is +1.4° C with an annual precipitation of ca. 1240 mm (Dragotă and Kucsicsa, 2011; Kucsicsa, 2013). Rainfall is highest, but most variable, in the summer and lowest in winter (Iezerul Pietrosul Meteorological Station; 47°35'2.18"N, 25° 1'26.80"E; 1785 m a.s.l.). The wind direction is predominantly from the south-west and north-east with an average multiannual wind speed between 3 and 4 m s^{-1}. In the winter, at high altitudes (above 1800 m), wind can reach speeds of over 35 m/s (Kucsicsa, 2013). According to Varga et al. (2016) the present dust fluxes in the Carpathian Basin range from 3.2 to 5.4 g m^{-2} yr^{-1} (dry deposition: 1.6–3.2 g m^{-2} yr^{-1}, wet deposition: 1.3–2.7 g m^{-2} yr^{-1}). Modelled dust fluxes in Romania range between 5–10 g m^{-2} yr^{-1} in the north and 2–5 g m^{-2} yr^{-1} in the south of the country (Tegen and Fung, 1995).

3. Material and methods

3.1. Fieldwork and radiocarbon dating

Parallel cores (in 100 cm segments) were extracted from the centre of the bog using a Russian corer. The cores were wrapped in plastic film, sealed for transportation and stored at 4°C. In this study only the top, ombrotrophic 450 cm of the peat core was used. The chronology of the master core was established on the basis of twelve AMS radiocarbon measurements of hand-picked plant macrofossils and unwashed bulk peat samples (CHRONO Centre in Queen’s University Belfast Radiocarbon Laboratory) and a ^{210}Pb profile (Faculty of Environmental Science, University of Babes Bolyai). For the details of the radiocarbon ages and age-depth

ACCEPTED MANUSCRIPT

modelling see (Feurdean et al., 2015; Panait et al., 2017).

3.2. Bulk density and loss on ignition

The organic matter and minerogenic content of the cores were estimated using loss on ignition (LOI) at 2 cm intervals (n=225). Samples of 4 cm^3 were extracted using a volumetric sampler. The sediment volume for the top of the profile was also measured by wet volumetric displacement. Peat samples of known weight and volume were placed in pre-weighed crucibles, dried for 12 hours at 105 °C in order to remove their water content, cooled and weighed again (Heiri et al, 2001). Bulk density (BD) was calculated by dividing the peat's dry mass by its wet volume. The samples were then heated at 550° C for 4 hours, cooled, and re-weighed in order to estimate their organic matter (OM) and minerogenic content (Heiri et al, 2001). Since inputs to ombrogenous peat bogs are atmospheric, the minerogenic content should reflect the input of sand and dust.

3.3. Grain size

We measured sample grain size into two ways: manual counting of particles and based on laser-based particle size analysis. Firstly, we estimated past aeolian sand input based on the manual size discrimination and counting of particles (ASD count) using a modified protocol of Björck and Clemmensen (2004). The ash resulting from the combustion of the samples at 550ºC was placed into Petri dishes, diluted with water and analysed using a Zeiss stereomicroscope (50x magnification). The original methodology requires the dissolution of the ash using 10% HCl, but we elected to replace the acid with water avoid the destruction of any carbonate particles. The profile was analysed at a resolution of 2 cm (n=225) and for each sample

ACCEPTED MANUSCRIPT

approximately 4 cm^3 was analysed. All the mineral particles were counted and divided into three grain size classes (100–200 µm, 200–300 µm, > 300 µm) representing fine to coarse sand. For each sample, the maximum diameter of grains was measured. To estimate dust sources, we also differentiated the mineral types into quartz, calcite and others based on their colour, lustre, cleavage and fracture.

Secondly, we used particle size analysis (PSA) to determine the clay, silt (proxy for dust) and sand fraction of the peat ash. This was carried out using a Horiba LA-960 Laser Particle Size Analyser. This instrument complies with standard procedures (ISO 13320, Particle size analysis — Laser diffraction methods) with a documented accuracy of 3% on the median of a broad distribution of standards with a precision of 0.1%. Repeat measurements (5 times) of each sediment sample were performed (after 1 minute of ultra-sonication) in order to minimise uncertainties. The resolution of the studied samples is the same as for the manual counting (n=225). Measured grain sizes were then transformed into the Udden-Wentworth grain-size classification (Wentworth, 1922). Particles sizes were divided into the following categories: clay, silt (very fine, fine, medium and coarse) and sand (very fine, fine, medium and coarse).

The atmospheric soil dust flux (ASD PSA) was calculated by multiplying the total silt fraction (3.9–63 µm), the peat accumulation rate (m a^{-1}) and the bulk density (g m^{-3}). For the atmospheric sand flux (ASI PSA) we used the sand particle fraction (63–2000 µm). In addition, we calculated the aeolian sand influx (ASI counted; grains cm^{-2} yr^{-1}) by multiplying the total grains concentration (grains cm^{-3}) by the peat accumulation rate (cm yr^{-1}).

3.4 X-ray fluorescence (XRF)

ACCEPTED MANUSCRIPT

Peat geochemistry was investigated employing a Niton XL3t 900 XRay Fluorescence analyser (fpXRF) on powdered material. NCS DC73308 was employed as a Certified Reference Material (CRM). We used sample concentrations of titanium (Ti), a lithogenic, conservative element to estimate the flux of dust (Shotyk et al. 2002). The detection limit on the analyser for the element of interest (Ti) is report as 6 mg kg^{-1}. Multiple measurements with different analysis periods were made to ensure reproducibility.

The atmospheric soil dust (ASD Ti) flux was calculated using bulk peat concentrations of Ti (µg g^{-1}), the concentration of the Ti in the upper continental crust (UCC), the peat accumulation rate (cm yr^{-1}) and the bulk density of the peat (g cm^{-3}) (Shotyk et al., 2002). For the UCC concentration we used values from Rudnick and Gao (2003) who reported concentrations of 3837 µg g^{-1} for Ti.

3.5. Statistical and graphical software

We calculated correlation coefficients and p values to denote the direction and strength of the relationship between dust deposition as determined from this study and climate, vegetation and fire taken from the published datasets from the same site. Testate amoebae based-depth to water table estimates (Diaconu et al., 2017) and Sphagnum $\delta^{13}C$ (Panait et al., 2017) were used as a proxy for climate, pollen (Feurdean et al., 2017) was used as a proxy for tree cover and human impact, and charcoal (Feurdean et al., 2017) as a proxy for disturbance by fire. Down sampling, or linear interpolation, was performed to account for differences in temporal resolution in the datasets.

Classical cluster analysis was employed to identify significant temporal changes in dust and sand influxes. Homogeneity test for time series using the Pettit test was

ACCEPTED MANUSCRIPT

employed to determine whether the calculated dust flux may be considered as homogeneous over time and to determine the timing of high amplitude changes in fluxes.

4. RESULTS

4.1 Age depth model

The total length of the profile is about 528 cm with a maximum age of 11,700 cal. yr BP in the base of the profile (Fig. 2). Throughout the profile the peat accumulation rate was largely uniform (0.3 ± 0.02 mm year^{-1}) until 1400 cal. yr BP; thereafter accumulation increased to 1.3 ± 0.3 mm year^{-1}. In this study we have used only the top 450 cm as the bottom part of the profile is not ombrogenous. The entire chronology of the Tăul Muced peat bog is presented and discussed in detail in Panait et al. (2017).

4.2 Bulk density and minerogenic content

Bulk density values ranged between 0.03 and 0.15 g/cm3 (mean 0.08 ± 0.02 g/cm3). BD was the highest (~0.15 ± 0.02 g/cm3) between 4500 and 2500 cal. yr BP and lowest (~0.06 ± 0.01 g/cm3) between 1400 and 200 cal. yr BP (Fig. 3).

The minerogenic content of samples ranged from 0.30 to 9.05% (mean 2.37 ± 1.13%). Higher minerogenic content was found during the following periods: 4050–3650, 3200–2200, 1550–1400, 1150–1050, 950–850, 150 – -66 cal. yr BP (Fig. 3).

4.3 Grain size

4.3.1 Manually counted sand particles

Observations under stereomicroscope revealed that the sand particles in the peat core consisted mainly of quartz (20-100%; mean 92 ± 12 %), followed by calcite

ACCEPTED MANUSCRIPT

(0-50%; mean 5 ± 8 %), while other minerals such as mica (biotite and muscovite), feldspar, sulphur, magnetite and olivine occurred with a comparatively low abundance (0 - 67%; mean 4 ± 9 %). However, the proportion of the mineral types found varied over time with cluster analysis showing four statistically significant changes at 5900, 3350, 2100 cal. yr BP (Table 1).

The total number of grains counted ranges from 0 to 70 grains cm^{-3} (mean 12 ± 5 grains cm^{-3}) with particularly variable values between 7800 and 2800 cal. yr BP (Fig. 3). The size of the sand particles ranged from 100 to 1200 µm (median of 400 ± 350 µm); with the most common size classes being 100-200 µm and 200-300 µm (Fig. 3, Table 2). Intervals with elevated numbers of sand particles were recorded at 7100–6700, 6400–6250, 5900–6100, 5500–5300, 4400–4250, 3500–3300, 3100–2700, 1600–1400, 1250–1100, 1000–800 cal. yr BP and over the last 200 years (Fig. 3). Larger particles sizes (diameter larger than 500-600 µm) were recorded more abundantly at about 6800, 4300, 4000, 3400, 3000, 900 and 25 cal. yr BP (Fig. 3).

4.3.2 Particle size analysis using laser diffraction

Laser-based particles size determination ranged from clay to coarse sand (Table 3, Fig. 4). The majority of the particles were silt sized ranging from fine to coarse silt (7.8–63 µm). The median particle size ranged from 10 to 37 µm (21 ± 5 µm). The sand and coarse silt fraction was highest between 7800 and 6100 cal. yr BP, 3300–1900 cal. yr BP and over the last 100 years, whereas finer particles (clay to fine silt) values were more abundant between 5900–4400 and 1800–300 cal. yr BP.

The sand flux from PSA varied between 0 and 2054 mg m^{-2} yr^{-1}; mean 181 ± 271 mg m^{-2} yr^{-1}(Fig. 6). The ASI counted ranged from 0 to 8 grains cm^{-2} yr^{-1} with a mean of 0.6 ± 0.8 grains cm^{-2} yr^{-1} (Fig. 6). The profiles of the two calculated sand fluxes

ACCEPTED MANUSCRIPT

show both similar and divergent trends (Fig. 6). The higher values in both the manually and instrument–based sand fluxes occurred between 7200–6600, 4150–2600, 1500–1000 cal. yr BP and in the last 200 years, whereas the period where they diverged the most was 4150–2600 cal. yr BP with a high instrument–based PSA, but a low value counted manually).

4.4 Geochemical analysis (Ti)

The concentration of Ti ranged between 39 and 1860 mg kg^{-1} (average 390 ± 287 mg kg^{-1}, Fig. 5). The concentration of this element showed the highest values during the following periods: 5500–5300, 4350–3700, 3100–2700, 2100–1900, 1600–1400, 1300–1100, 1000–900 cal. yr BP and the last 100 years.

The dust flux calculated from Ti concentrations (ASD Ti) shows a large variability throughout the profile (min 0 µg m^{-2} yr^{-1}, max 86 µg m^{-2} yr^{-1}; median 8 ± 10 µg m^{-2} yr^{-1}), with higher values recorded between 7100–6600, 3700–4100, 3700–4100, 3200–2500 and 1500–1000 cal. yr BP, and in the last 200 years (Fig. 6). The dust flux estimates based on PSA (ASD PSA) show a similar trend to those derived from ASD Ti (82 to 10648 mg m^{-2} yr^{-1}; mean 1294 ± 1367 mg m^{-2} yr^{-1}; Fig. 6).

4.5 Statistical analysis

Homogeneity tests indicate a clear change at 4150 and 150 cal. yr BP in the deposition of aeolian fluxes with a confidence level of 0.05 and a p value of <0.0001. Based on the classical clustering with paired group algorithm and Euclidean similarity index on aeolian fluxes and also the homogeneity tests we have divided the entire record into 4 distinct zones: Zone a (7800–4150 cal. yr BP) is characterised by a lower deposition of dust, but high influxes of sand. Zone b (4150–2300 cal. yr BP) is defined

ACCEPTED MANUSCRIPT

by the intense deposition of both sand and dust. In zone c (2300–150 cal. yr BP) overall the aeolian deposition is relatively low with several short periods of intensifications. The last zone, the zone d (150 cal. yr BP – present), is characterised by the very intense deposition of both sand and dust.

Using multiple linear regressions, we found that a combination of all parameters (tree cover, DTW, $\delta^{13}C$, charcoal) explains the dust deposition (R=0.69). The regression based on the clustering and homogeneity test were performed separated on the 7800–150 cal. yr BP and the last 200 years periods, as the pollen record show that the latter was strongly impacted by human activity (Fig. 5). The regression analyses showed that during the period 7800–150 cal. yr BP the dust flux had the highest correlation with DTW for all parameters (R=0.43), which indicates that the climate had the most impact on deposition in this period. However, over the last 200 years dust showed the highest regression coefficient with tree cover (R=0.58), which suggests that the dust influx was stronger influenced by the degree of regional to local land cover, especially the marked regional deforestation over from the last two centuries.

5. Discussion

The estimates of aeolian deposition at Tăul Muced cover the last 7800 years and show a good similarity between the sand and dust fluxes (r >0.70), particularly over the last 4000 years (Fig. 6). This suggests more common drivers and sources in aeolian fluxes in the more recent part of the record. Cluster analysis shows that aeolian deposition has varied considerably throughout the mid to late Holocene with distinct periods characterised by a high aeolian input around 7800–6800, 6550–5000, 3900–3500, 2900–2300, 1250–600 and over the last 200 cal. yr BP (Fig. 5, 6). Below, we

ACCEPTED MANUSCRIPT

discuss the trends in dust and sand particles observed in this peat core and consider the potential drivers of the changes in minerogenic input.

5.1 The influence of past climatic conditions and human impact on aeolian input

5.1.1 7800–4150 cal. yr BP: low deposition rates of dust; enhanced sand flux

The aeolian dust deposition was the lowest in the profile between 7800 and 4150 cal. yr BP (Fig.6). Sand influx on the other hand, shows enhanced values during this time interval in particular between 7100 – 6500 and 5500 – 4800 BP cal. yr BP with a rise in both dust and sand fluxes between 6400 and 6200 cal. yr BP (Fig. 6). Additionally, the two shorter–term intervals of high sand deposition were characterised by larger sand sized particles (Fig. 3). Climatically, the $\delta^{13}C$ isotope and depth to water table (DTW) record at this site show dry to moderately dry conditions during the entire 7800–4100 cal. yr BP interval, which suggests that dry conditions lead to higher erosion rates (Panait et al., 2017). The parallel increase in fire activity with sand fluxes at the study site (Feurdean et al., 2017) may also suggest greater erosion and localised sand deposition following forest disturbance by fire. The mineralogy of the sand particles shows the dominance of quartz, but with an increased abundance of other minerals compared with previous, calmer periods. This may possibly indicate a change in source, which could reflect a shift in wind direction or the opening up of a new source area following changes in vegetation cover or human activity (Fig. 3).

An increase in both dust and sand fluxes is recorded between 6400 and 6200

ACCEPTED MANUSCRIPT

cal. yr BP, and the high maximum grain size (500 to 700 μm), possibly indicates a period of high velocity winds (Fig. 5). A small increase in the dust flux was also recorded at 6200–6100 cal. yr BP at Mohoş, Romania approximate 200 km away (Longman et al., 2017). In addition, Le Roux et al. (2012) detected a peak in Ti concentration in a peat core from the Jura Mountains at this time, which was assigned to volcanic eruptions in Iceland or Faroe Island, although this hypothesis was not supported by the values of εNd. Therefore, while a dust flux intensification appears to have occurred on a regional scale at this time, the triggers for this event are less obvious. (Fig. 7).

5.1.2 4150–2300 cal. yr BP: increased deposition of sand and dust

This period was characterised by a marked increase in aeolian particle deposition. Whilst ASD Ti suggests the possibility of a stronger input from greater distances, the median grain size and the high values of maximum grain size also indicate enhanced local erosion and transport, particularly from 3500 cal. yr BP onwards (Figs. 5, 7). The particle size distribution shows that during this period the sand content is generally high while the finer fraction reduced. From a mineralogical point of view, increased ASD Ti fluxes were characterised by a greater range of particles types, comprising quartz, calcite and others, whereas during more quiescent periods, quartz dominated the sand particle record (Fig. 3). Overall, these characteristics do not support the indication that the ASD Ti input was predominantly from regional sources (Fig. 4). Local climate conditions were mainly wet, as indicated by a high–water table and enriched values of $\delta^{13}C$ (Panait et al., 2017). Cooler mean summer temperatures during this period were reconstructed locally (Feurdean et al., 2008; Diaconu et al., 2017) and over a wide region (Samartin et al., 2017). There were

ACCEPTED MANUSCRIPT

no major changes in the local tree cover, and disturbance by fire or human impacts to explain such a significant rise in aeolian particles (Feurdean et al., 2017; Grindean et al., 2019). However, enhanced deforestation and the use of fire in surrounding mountain areas are apparent from 3500–3000 cal. yr BP (Feurdean et al., 2010; 2016; Tanţău et al., 2011, 2014a; Fărcaş et al., 2013; Geantă et al., 2014; Florescu et al., 2018), coincident with this marked increase in sand influx. On a regional scale, however, pollen records from lowland areas show an earlier onset of larger–scale deforestation, which corresponds with the rise in aeolian flux at TM (Tanţău et al., 2006; Magyari et al., 2010; Feurdean et al., 2015; 2018). Archaeologically, this period of enhanced input of aeolian particles and human impact corresponds to the Bronze Age and characterised by key technological developments (Sherratt, 1981, Cârciumaru, 1995). The introduction of the metal plough was the main cause for the greater susceptibility of agricultural fields to wind–driven soil erosion (Goossens et al., 2001; Funk et al., 2008; Nykamp et al. 2017). Collectively, the combined results appear to indicate that intensification in land use initiated in the lowlands, gradually extending to high elevations, could have led to higher concentrations of particulates in the atmosphere in this period.

A regional increase in the dust fluxes from 4000–3700 and 3600-3200 cal. yr BP is also visible in peat–based dust records from Belgium, Romania, Switzerland and Poland (Fig. 7) (Le Roux et al., 2012; Tudyka et al. 2017). Magny et al. (2009) suggested dry climatic conditions during the period 4100–3950 cal. yr BP, which may have triggered higher wind erosion and the transport of high levels of dust over short period from more arid regions.

5.1.3 2300–150 cal. yr BP: low deposition rates of dust and sand with

ACCEPTED MANUSCRIPT

periodic increases in both

This period was characterised by marked fluctuations in the flux of sand and dust particle deposition, and a higher concentration of finer particles (very fine and fine silt), suggesting a possible increased input from a regional source (Fig. 4, 5). The most evident short–term increases in all aeolian inputs were recorded at 1600–1400, 1300–1100 and 1000–900 cal. yr BP. They were accompanied by rapid changes in the mineralogical composition with a mixed mineralogy suggesting erosion of a greater range of rock types during this period (Fig. 5). The testate amoeba record at TM indicates that the bog was moderately wet during most periods of high aeolian influx (Diaconu et al., 2017). This could suggest that aeolian deposition was triggered by a wet deposition, or that the wet periods were also characterised by strong winds that could have increased deposition. The pollen record at this site shows a steady decline in tree cover and an increase in fire activity, especially between 1500-1000, and 400-200 cal. yr BP (Feurdean et al., 2017). A general pattern of increased deforestation and fire was observed at other sites in this region (Tanţău et al., 2011; 2014a; Geantă et al., 2014; Feurdean et al., 2016; Florescu et al., 2018), which may suggest that local to regional deforestation and disturbance by fire may have also contributed to the sand input and, at the same time, explain the diversity of particulate mineralogy.

In the Eastern Carpathians an increase in dust flux is recorded only later at about 1000 cal. yr BP (Longman et al., 2017). Moist conditions, linked to a stronger influence of maritime air masses in the study region between 1050 – 750 cal. yr BP, coincide with the Medieval Climatic Anomaly (MCA) in this region (Feurdean et al., 2015; Florescu et al., 2017; Persoiu et al., 2017; Persoiu and Persoiu 2019). These findings contrast with the lower dust fluxes found in Western and Northern Europe in the same period (de Jong et al 2006, 2007; De Vleeschouwer et al.,2009; Le Roux et al., 2012).

ACCEPTED MANUSCRIPT

This dissimilarity, between the sites from eastern Europe and those in central and northern parts of Europe, may be explained by the greater influence of Saharan and Mediterranean air masses on Eastern Europe during MCA. However, tropical Africa recorded a drought in the MCA, which suggests the potential for a higher erosion rate in the MCA period, which agrees well with this record of aeolian influx (Verschuren, 2004). Interestingly, we found a significant drop in sand and dust input between 650 – 150 cal. yr BP coinciding with the Little Ice Age, which, together with smaller grain sizes, indicates slower wind speeds and lower erosion rates (Fig. 6). The particle size range (mainly very fine and fine silt) suggests that the input was primarily from regional sources. A decline in the fluxes of terrigenous geochemical elements is visible over a wider area in the northern Carpathians (Haliuc et al., 2016; Florescu et al., 2017), whereas the reconstructed climate conditions at the site and close to the site were dry (Feurdean et al., 2008; 2015). A decline in dust flux during the LIA is also recorded at Mohoş peatbog (Longman et al., 2017), but results contrast with the pattern of increasing aeolian influx in peat bogs from Western Europe (De Vleeschouwer et al.,2009, Le Roux et al., 2012). We suggest that Saharan air mass trajectories (Gagen et al., 2016), that transport the most dust, may have migrated more towards central and Western Europe during the LIA and resulted in a correspondingly lower dust fluxes over Eastern Europe.

5.1.4 Marked anthropogenic–enhancement of sand and dust deposition in the last 200 years.

The last 200 years show the most evident enhancement in sand and dust deposition of up to 10 times more than the average for the entire profile (Fig. 6). The increase in maximum grain size and concentration of larger particles suggest higher

ACCEPTED MANUSCRIPT

erosion rates (Fig. 5). The pollen record at Tăul Muced (Feurdean et al., 2017), and at neighbouring mountain sites (Tanţău et al., 2011; 2014a; Geantă et al., 2014; Feurdean et al., 2016; Florescu et al., 2017), show marked deforestation trends, increased alpine grassland cover and grazing activity. These activities could have enhanced erosion rates and therefore the influx of sand and dust particles at this site. It is documented that increase in farming activity worldwide over the last two centuries (Olofsson et al. 2011), has resulted in land degradation and consequently higher soil erosion rates and concentrations of dust in the atmosphere (De Vleeschouwer et al., 2009; Marx et al., 2011; Le Roux et al., 2012; Fiałkiewicz–Kozieł et al., 2016; Hutchinson et al., 2015; Haliuc et al., 2018).

5.2 Comparison with regional trends in aeolian flux

5.2.1 Sand fluxes

Comparison of the reconstructed aeolian sand deposition from this study with similar data from NW Europe (Sweden) shows few common trends (Björck and Clemmensen, 2004; de Jong et al. 2006) (Supp 1). In general, previous studies have used manual counting methods. In NW Europe, most sites are coastal, located in close proximity to the sand sources and associate the influx of these coarse–grained particulates with winter storms. In contrast, the input of sand at our site seems to be stronger correlated with higher erosion rates following local deforestation and fires. This suggests that local factors have influenced the erosion and deposition of coarser particles resulting in divergent trends between regions.

5.3.2 Dust fluxes

ACCEPTED MANUSCRIPT

In terms of dust deposition, a regional comparison of past dust fluxes across Europe shows that the earlier part of this profile (7800–3600 cal. yr BP) shows similarities with records from Romania but also on a wider region in Central and NW Europe (Table 4). This suggests a possible common mechanism driving early to mid-Holocene aeolian deposition over Western and Eastern Europe. However, from ca. 3600 cal. yr BP, the regional pattern in aeolian deposition diverges strongly, especially in dust fluxes and suggests the greater influence of either local climate conditions or anthropogenic impact. Gagen et al. (2016) demonstrated that the temperature contrast between northern and southern Europe could have caused a redistribution of precipitation and cloud cover linked to oscillations in the position of summer storm tracks. The consequences of this temperature contrast for atmospheric conditions could explain this apparently strongly divergent aeolian deposition patterns between Western and Eastern Europe.

5.3 Comparison of methods: advantages and disadvantages

In this study we tested three different methods to determine sand and dust particles deposition over time. These include: 1) using elemental variations in Ti; 2) the determination of particle size classes through manual counting of sand particles; and 3) instrument-based analysis of the particle size distribution using laser diffraction. Below we discuss the advantages and disadvantages associated with each of the three methods.

We found that the geochemistry (Ti) based aeolian soil dust estimates (ASD; $\mu g*m^{-2}*a^{-1}$) have the advantage of providing a rapid method of calculating dust fluxes. However, we identify three main disadvantages with this method. Firstly, it cannot provide information on grain size. Secondly, it does not allow a quantitative estimate

ACCEPTED MANUSCRIPT

of total dust influx since dust flux is derived via chemical composition, which can change according to source material. Thirdly, it does not permit any determination of whether the geochemical fingerprint reflects regional dust or local particle sources. Although the contribution of local particles to the total aeolian flux is lower, and imprints less on the geochemical composition, disentangling changing regional from local particles contributions to influxes is essential.

We found the aeolian sand input (ASI counted; grains m^{-2} yr^{-1}), calculated on the basis of manually counted particles to be a powerful tool for the investigation of past sand influxes and changes in the mineralogy of sand particles over time. However, because the identified and counted sand grains have a range of sizes, shapes and densities, it remains difficult to quantify the total number of grains, particularly of finer material, which is more difficult to isolate. Hence, this method may strongly underestimate smaller size particles (<100µm). Another disadvantage of this method is that the estimate is not directly comparable to the other estimates of aeolian influxes due to the different units of measurement used (grains m^{-2} yr^{-1}vs µg m^{-2} yr^{-1}, Table 4).

Our third method of estimating particulate fluxes i.e., ASD PSA (mg m^{-2} yr^{-1}) and ASI PSA (mg*m^{-2}*a^{-1}) determined via laser diffraction particle size analysis provides a quantification of all particles contained in peat; ranging from clay to coarse sand. An additional advantage of this method is the quantitative basis on which the dust flux is determined. However, a disadvantage of this approach may be that, during sample preparation and the measurement procedure, some larger particles may become disaggregated leading to the formation of smaller grains and a potential overestimation of this particle size fraction.

In summary, all the methods employed have some disadvantages; however,

ACCEPTED MANUSCRIPT

these can be overcome by a combined approach. We suggest that laser-based particle size analysis, used in combination with the other two methods can provide a more detailed understanding of past aeolian influxes, than the geochemistry-based or manual counting particle size estimates alone. However, the advantage of manual counting is that this approach additionally allows the quantification of the mineralogy of the sand over time, whereas a key benefit of laser-based particle size analysis is that provides a quantification of the full particle size range.

6. Conclusions

This multi-proxy study of the Tăul Muced ombrotrophic peat profile, Romania, provides a detailed reconstruction of Holocene aeolian dust and sand fluxes in CE Europe. The comparative approach, using laser-based particle size analysis, with more established methods (geochemistry and the manual counting of sand particles) provides a more detailed understanding of past aeolian influxes than geochemistry-based or manual estimates alone.

This study identified several changes in the trend of aeolian fluxes (dust and sand) over the last 7800 years: 7800–4150 cal. yr BP – generally low dust fluxes with the periodic intensification of sand fluxes; 4150–2300 cal. yr BP – intense deposition of both dust and sand; 2300–150 cal. yr BP – rapid shifts in deposition with both highs and lows; the last 200 years – the highest magnitude of both sand and dust fluxes. In general, all the calculated dust and sand fluxes show similar trends, but the sand record indicates that during some periods (e.g., 7100–6800, 5500–4800, 4400–4200 cal. yr BP) storm activity appears to have affected the area supplying material from a relatively close source. The variability of aeolian fluxes appears to have been related to the combined influence of climatic conditions and anthropogenic impact

ACCEPTED MANUSCRIPT

(deforestation and fire) during the most periods; the role of anthropogenic driver becoming more dominated in more recent times.

This record shows similarities, as well differences, compared to records of dust fluxes published from Western and Central Europe. Overall, we found a stronger European scale agreement between 6300 and 3500 cal. yr BP, and an increased dissimilarity in the last 3500 years, which may either imply distinct climate conditions or anthropogenic impacts.

Acknowledgements

This work was supported by the CNCS – UEFISCDI [PN-II-RU-TE-2014-4-2445] and [PN-III-P4-ID-PCE-2016-0711]. AP thanks Matthew Dennis from the University of Salford for help during laboratory work. We thank the anonymous reviewers for their careful reading of our manuscript and their many insightful comments and suggestions.

References

Akinyemi, F. O., Hutchinson, S. M., Mîndrescu, M., & Rothwell, J. J., 2013. Lake sediment records of atmospheric pollution in the Romanian Carpathians. Quaternary International, 293, 105-113.

Allan, M., Roux, G. Le, Piotrowska, N., Beghin, J., Javaux, E., Mattielli, N., & Verheyden, S., 2013. Mid- and late Holocene dust deposition in western Europe: the Misten peat bog (Hautes Fagnes – Belgium), 2285–2298. http://doi.org/10.5194/cp-9-2285-2013

ACCEPTED MANUSCRIPT

Bercia I., Kräutner H. & Mureşan M., 1976. PreMesozoic Metamorphites of the East Carpathians. Anuarul Institutului de Geologie şi Geofizică al R.S. România, 50: 37-50.

Björck, S., & Clemmensen, L. B., 2004. Aeolian sediment in raised bog deposits, Halland, SW Sweden: a new proxy record of Holocene winter storminess variation in southern Scandinavia?. The Holocene, 14(5), 677-688.

Cârciumaru M. 1995. Paleoethnobotanica. Studii în preistoria și protoistoria României. Istoria agriculturii din România. Bucureşti (in Romanian)

Cristea G., Cuna S.M., Fărcaş S., Tanţău I., Dordai E., Măgdaş D.A., 2014. Carbon isotope composition as indicator for climatic changes during the middle and late Holocene in a peat bog from Maramureş Mountains (Romania). The Holocene 24(1), 15-23.

Davis, B. A., Brewer, S., Stevenson, A. C., & Guiot, J., 2003. The temperature of Europe during the Holocene reconstructed from pollen data. Quaternary Science Reviews, 22(15), 1701-1716.

De Jong, R., & Björck, S., 2006. Storminess variation during the last 6500 years as reconstructed from an ombrotrophic peat bog in Halland, southwest Sweden. *Journal of Quaternary …*. http://doi.org/10.1191/0959683604hl746rp

De Jong, R. de, Schoning, K., & Björck, S., 2007. Increased aeolian activity during climatic regime shifts as recorded in a raised bog in south-west Sweden during the past 1700 years. *Climate of the Past Discussions*, *3*(1), 383–408. http://doi.org/10.5194/cp-3-411-2007

De Vleeschouwer, F., Piotrowska, N., Sikorski, J., Pawlyta, J., Cheburkin, A., Le Roux, G., Lamentowicz M., Fagel N., Mauquoy, D. 2009. Multiproxy evidence of `Little

Ice Age' palaeoenvironmental changes in a peat bog from northern Poland. *The Holocene*, *19*(4), 625–637. http://doi.org/10.1177/0959683609104027

Denton, G. H., & Karlén, W. 1973. Holocene climatic variations—their pattern and possible cause. Quaternary Research, 3(2), 155IN1175-174IN2205.

Diaconu, A.C., Tóth, M., Lamentowicz, M., Heiri, O., Kuske, E., Tanţău, I., Panait, A.M., Braun, M., Feurdean, A., 2017. accepted for publication. How warm? How wet? 7500 years of hydroclimate reconstructions in the northern Carpathians, Romania. Palaeogeography, Palaeoclimatology, Palaeoecology, 482, 1-12.

Dragotă, C.S., Kucsicsa, G., 2011. Global climate change-related particularities in the Rodnei Mountains National Park. Carpathian J. Earth Environ. Sci. 6, 43–50.

Dreibrodt, S., & Wiethold, J. 2015. Lake Belau and its catchment (northern Germany): A key archive of environmental history in northern central Europe since the onset of agriculture. The Holocene, 25(2), 296-322.

Fărcaş, S., Tanţău, I., Mîndrescu, M., & Hurdu, B., 2013. Holocene vegetation history in the Maramureş mountains (Northern Romanian Carpathians). Quaternary International, 293, 92-104.

Feurdean, A., 2005. Holocene forest dynamics in northwestern Romnania. The Holocene, 15(3), 435-446.

Feurdean, A., Klotz, S., Mosbrugger, V., Wohlfarth, B., 2008. Pollen-based quantitative reconstruction of Holocene climate variability in NW Romania. Palaeogeography, Palaeoclimatology, Palaeoecology 260: 494-504.

Feurdean, A., Willis, K. J., Parr, C. L., Tanţău, I., & Fărcaş, S., 2010. Post-glacial patterns in vegetation dynamics in Romania: homogenization or differentiation?. Journal of Biogeography, 37(11), 2197-2208.

Feurdean A., Liakka J., Vannière B., Marinova E., Hutchinson S.M., Mosburgger V., Hickler T., 2013. 12,000-Years of fire regime drivers in the lowlands of Transylvania (Central-Eastern Europe): a data-model approach, Quaternary Science Reviews, Volume 81

Feurdean, A., Gałka, M., Kuske, E., Tanţău, I., Lamentowicz, M., Florescu, G., Liakka, J., Hutchinson, S.M., Mulch, A. & Hickler, T., 2015. Last Millennium hydro-climate variability in Central–Eastern Europe (Northern Carpathians, Romania). The Holocene, 25 (7): 1179–1192.

Feurdean, A., Gałka, M., Tanţău, I., Geantă, A., Hutchinson, S. M., & Hickler, T., 2016. Tree and timberline shifts in the northern Romanian Carpathians during the Holocene and the responses to environmental changes. Quaternary Science Reviews, 134, 100-113.

Feurdean, A., Florescu, G., Vannière, B., Tanţău, I., O'Hara, R. B., Pfeiffer, M., Hutchinson, S.M., Gałka, M., Moskal-del Hoyo, M., & Hickler, T., 2017. Fire has been an important driver of forest dynamics in the Carpathian Mountains during the Holocene. Forest Ecology and Management, 389, 15-26.

Florescu, G., Hutchinson, S. M., Kern, Z., Mindrescu, M., Cristea, I. A., Mihăilă, D., Łokas D., & Feurdean, A., 2017. Last 1000 years of environmental history in Southern Bucovina, Romania: A high resolution multi-proxy lacustrine archive. Palaeogeography, Palaeoclimatology, Palaeoecology, 473, 26-40.

Fiałkiewicz-Kozieł, B., Smieja-Król, B., Frontasyeva, M., Słowiński, M., Marcisz, K., Lapshina, E., ... & Laggoun-Défarge, F., 2016. Anthropogenic-and natural sources of dust in peatland during the Anthropocene. Scientific Reports, 6, 38731.

Field, J. P., Belnap, J., Breshears, D. D., Neff, J. C., Okin, G. S., Whicker, J. J., Painter, T. H., Ravi, S., Reheis, M. C. and Reynolds, R. L., 2010. The ecology of dust.

ACCEPTED MANUSCRIPT

Frontiers in Ecology and the Environment, 8: 423–430. doi:10.1890/090050

Florescu, G., Vannière, B., & Feurdean, A. 2018. Exploring the influence of local controls on fire activity using multiple charcoal records from northern Romanian Carpathians. Quaternary International.

Funk, R., Reuter, H.I., Hoffmann, C., Engel, W., Öttl, D., 2008. Effect of moisture on fine dust emission from tillage operations on agricultural fields. Earth Surf. Process. Landf. 33, 1851–1863.

Gabrielli, P., Wegner, A., Petit, J.R., Delmonte, B., De Deckker, P., Gaspari, V., Fischer, H., Ruth, U., Kriews, M., Boutron, C., Cescon, P., and Barbante, C 2010. A major glacial-interglacial change in aeolian dust composition inferred from Rare Earth Elements in Antarctic ice, Quaternary Sci. Rev., 29, 265–273.

Gagen, M. H., Zorita, E., McCarroll, D., Zahn, M., Young, G. H., & Robertson, I., 2016. North Atlantic summer storm tracks over Europe dominated by internal variability over the past millennium. Nature Geoscience.

Gałka, M., Tanţău, I., Ersek, V., Feurdean, A., 2016. A 9000year record of cyclic vegetation changes identified in a montane peatland deposit located in the Eastern Carpathians (Central-Eastern Europe): Autogenic succession or regional climatic influences?, In Palaeogeography, Palaeoclimatology, Palaeoecology, Volume 449, 52-61.

Geantă, A., Gałka, M., Tanţău, I., Hutchinson, S. M., Mîndrescu, M., & Feurdean, A., 2014. High mountain region of the Northern Romanian Carpathians responded sensitively to Holocene climate and land use changes: A multi-proxy analysis. The Holocene, 24(8), 944-956.

Goossens, D., Gross, J., Spaan, W., 2001. Aeolian dust dynamics in agricultural land areas in Lower Saxony, Germany. Earth Surf. Process. Landf. 26, 701–720.

ACCEPTED MANUSCRIPT

Goudie, A., & Middleton, N. J., 2006. Desert dust in the global system. Springer Science & Business Media.

Grindean, R., Tanţău, I. and Feurdean, A., 2019. Linking vegetation dynamics and stability in the old-growth forests of Central Eastern Europe: Implications for forest conservation and management. Biological Conservation, 229, pp.160-169.

Grousset, F. E. and Biscaye, P. E., 2005. Continental aerosols, isotopic fingerprints of sources and atmospheric transport: a review, Chem. Geol., 222, 149–167.

Haliuc, A., Hutchinson, S. M., Florescu, G., & Feurdean, A., 2016. The role of fire in landscape dynamics: An example of two sediment records from the Rodna Mountains, northern Romanian Carpathians. Catena, 137, 432-440.

Haliuc, A., Feurdean, A., Mîndrescu, M., Frantiuc, A., & Hutchinson, S. M. 2018. Impacts of forest loss in the eastern Carpathian Mountains: linking remote sensing and sediment changes in a mid-altitude catchment (Red Lake, Romania). Regional Environmental Change, 1-15.

Hammer, O., Harper, D.A.T. & Ryan, P.D., 2001. PAST: Paleontological statistics software package for education and data analysis. Palaeontologia Electronica, 4 (1): 1-9.

Heiri, O., Lotter, A. F., & Lemcke, G., 2001. Loss on ignition as a method for estimating organic and carbonate content in sediments: reproducibility and comparability of results. Journal of paleolimnology, 25(1), 101-110.

Hutchinson S.M., Akinyemi F.O, Mîndrescu M., Begy R., Feurdean A., 2015. Recent sediment accumulation rates in contrasting lakes in the Carpathians (Romania): impacts of shifts in socio-economic regime. Regional Environmental Change, DOI: 10.1007/s10113-015-0764-7

Jiménez-Espejo, F.J., García-Alix, A., Jiménez-Moreno, G., Rodrigo-Gámiz, M.,

ACCEPTED MANUSCRIPT

Anderson, R.S., Rodríguez-Tovar, F.J., Martínez-Ruiz, F., Giralt, S., Huertas, A.D. and Pardo-Igúzquiza, E., 2014. Saharan aeolian input and effective humidity variations over western Europe during the Holocene from a high altitude record. Chemical Geology, 374, pp.1-12.

Jung, E. & Shao, Y. P., 2006. An intercomparison of four wet deposition schemes used in dust transport modelling. Global and Planetary Change, 52, 248-6.

Kalińska-Nartiša, E., Nartišs, M., Thiel, C., Buylaert, J. P., & Murray, A. S. 2015. Late-glacial to Holocene aeolian deposition in northeastern Europe–The timing of sedimentation at the Iisaku site (NE Estonia). Quaternary International, 357, 70-81.

Kohfeld, K. E., & Harrison, S. P. 2001. DIRTMAP: the geological record of dust. Earth-Science Reviews, 54(1-3), 81-114.

Kok, J. F., Parteli, E. J., Michaels, T. I., & Karam, D. B. 2012. The physics of wind-blown sand and dust. Reports on Progress in Physics, 75(10), 106901.

Kräutner H.G., Kräutner F. & Szasz, L. 1982. Geological map of Romania 1:50,000, sheet 20a - Pietrosul Rodnei. Geological Institute of Romania, Bucharest.

Kucsicsa G., 2013. Parcul national muntii Rodnei relatii om – mediu. Academia Română Editura Universitara, Bucuresti. DOI: 10.5682/9786065916098

Kylander, M. E., Bindler, R., Martínez Cortizas, A., Gallagher, K., Mörth, C. M., and Rauch, S., 2013. A novel geochemical approach to paleorecords of dust deposition and effective humidity: 8500 years of peat accumulation at Store Mosse (the “Great Bog”) Sweden, Quarternary Sci. Rev., 69, 69–82.

Kylander, M.E., Martínez-Cortizas, A., Bindler, R., Greenwood, S.L., Mörth, C.M. and Rauch, S., 2016. Potentials and problems of building detailed dust records using

ACCEPTED MANUSCRIPT

peat archives: An example from Store Mosse (the “Great Bog”), Sweden. Geochimica et Cosmochimica Acta, 190, pp.156-174.

Kylander, M. E., Martínez-Cortizas, A., Bindler, R., Greenwood, S. L., Mörth, C. M., & Rauch, S. 2016. Potentials and problems of building detailed dust records using peat archives: An example from Store Mosse (the “Great Bog”), Sweden. Geochimica et Cosmochimica Acta, 190, 156-174.

Lambert, F., Bigler, M., Steffensen, J. P., Hutterli, M., and Fischer, H., 2012. Centennial mineral dust variability in high-resolution ice core data from Dome C, Antarctica, Clim. Past, 8, 609–623, doi:10.5194/cp-8-609-2012

Lawrence, C. R., & Neff, J. C., 2009. The contemporary physical and chemical flux of aeolian dust: A synthesis of direct measurements of dust deposition. Chemical Geology, 267(1), 46-63.

Le Roux, G., Fagel, N., De Vleeschouwer, F., Krachler, M., Debaille, V., Stille, P., ... & Shotyk, W., 2012. Volcano-and climate-driven changes in atmospheric dust sources and fluxes since the Late Glacial in Central Europe. Geology, 40(4), 335-338.

Longman, J., Veres, D., Ersek, V., Haliuc, A. and Wennrich, V., 2019. Runoff events and related rainfall variability in the Southern Carpathians during the last 2000 years. Scientific Reports, 9(1), p.5334.

Longman, J., Veres, D., Ersek, V., Salzmann, U., Hubay, K., Bormann, M., Wennrich V. & Schäbitz, F., 2017. Periodic input of dust over the Eastern Carpathians during the Holocene linked with Saharan desertification and human impact. Climate of the Past, 13(7), 897.

ACCEPTED MANUSCRIPT

Magny, M., Vannière, B., Zanchetta, G., Fouache, E., Touchais, G., Petrika, L., ... & Arnaud, F., 2009. Possible complexity of the climatic event around 4300—3800 cal. BP in the central and western Mediterranean. The Holocene, 19(6), 823-833.

Magyari, E. K., Chapman, J. C., Passmore, D. G., Allen, J. R. M., Huntley, J. P., & Huntley, B., 2010. Holocene persistence of wooded steppe in the Great Hungarian Plain. Journal of Biogeography, 37(5), 915-935.

Mahowald, N., Kohfeld, K., Hansson, M., Balkanski, Y., Harrison, S. P., Prentice, I. C., ... & Rodhe, H. 1999. Dust sources and deposition during the last glacial maximum and current climate: A comparison of model results with paleodata from ice cores and marine sediments. Journal of Geophysical Research: Atmospheres, 104(D13), 15895-15916.

Mann ME, Ammann CM, Bradley RS et al. .2003. On past temperatures and anomalous late-20th century warmth. EOS 84: 256.

Mann ME, Zhang Z, Rutherford S et al. (2009) Global signatures and dynamical origins of the Little Ice Age and Medieval Climate Anomaly. Science 326: 1256–1260

Marx, S. K., Kamber, B. S., McGowan, H. A., & Denholm, J., 2011. Holocene dust deposition rates in Australia's Murray-Darling Basin record the interplay between aridity and the position of the mid-latitude westerlies. Quaternary Science Reviews, 30(23), 3290-3305.

Middleton, N. J., Goudie, A. S., 2001. "Saharan dust: Sources and trajectories". Transactions of the Institute of British Geographers 26 (2): 165. doi:10.1111/1475-5661.00013.

Muhs, D. R., & Bettis, E. A., 2000. Geochemical variations in Peoria Loess of western Iowa indicate paleowinds of midcontinental North America during last glaciation. Quaternary Research, 53(1), 49-61.

ACCEPTED MANUSCRIPT

Nykamp, M., Knitter, D., Timár, G., Krause, J., Heeb, B. S., Szentmiklosi, A., & Schütt, B., 2017. Estimation of wind-driven soil erosion of a loess-like sediment and its implications for the occurrence of archaeological surface and subsurface finds–An example from the environs of Corneşti-Iarcuri, western Romania. Journal of Archaeological Science: Reports, 12, 601-612.

Olofsson, P., Kuemmerle, T., Griffiths, P., Knorn, J., Baccini, A., Gancz, V., Blujdea, V., Houghton, R.A., Abrudan, I.V. and Woodcock, C.E., 2011. Carbon implications of forest restitution in post-socialist Romania. Environmental Research Letters, 6(4), p.045202.

Panait, A., Diaconu, A., Galka, M., Grindean, R., Hutchinson, S. M., Hickler, T., Tanţău, I., & Feurdean, A., 2017. Hydrological conditions and carbon accumulation rates reconstructed from a mountain raised bog in the Carpathians: A multi-proxy approach. Catena, 152, 57-68.

Perşoiu, A., Ionita, M. and Weiss, H., 2019. Atmospheric blocking induced by the strengthened Siberian High led to drying in west Asia during the 4.2 ka BP event–a hypothesis. Climate of the Past, 15(2), pp.781-793.

Perșoiu, I. and Perșoiu, A., 2019. Flood events in Transylvania during the Medieval Warm Period and the Little Ice Age. The Holocene, 29(1), pp.85-96.

Pichevin, L., Cremer, M., Giraudeau, J., & Bertrand, P., 2005. A 190 ky record of lithogenic grain-size on the Namibian slope: Forging a tight link between past wind-strength and coastal upwelling dynamics. Marine Geology, 218(1), 81-96.

Rudnick, R.L. and Gao, S., 2003. The Composition of the Continental Crust. In: Holland, H.D. and Turekian, K.K., Eds., Treatise on Geochemistry, Vol. 3, The Crust, Elsevier-Pergamon, Oxford, 1-64.

Sahy, D., Săsăran, E. and Tămaş, T., 2008. Microfacies analysis of Upper Eocene

ACCEPTED MANUSCRIPT

shallow-water carbonates from the Rodnei Mountains (N Romania). Studia UBB Geologia 53: 13–24.

Samartin, S., Heiri, O., Joos, F., Renssen, H., Franke, J., Brönnimann, S., & Tinner, W., 2017. Warm Mediterranean mid-Holocene summers inferred from fossil midge assemblages. Nature Geoscience 10, 207–212.

Sapkota, A., 2006. Mineralogical, chemical, and isotopic (Sr, Pb) Composition of atmospheric mineral dusts in an ombrotrophic peat bog, Southern South America, PhD Thesis, Ruprecht-Karls- Universität, Heidelberg, Germany.

Sassen, K., DeMott, P.J., Prospero, J.M., Poellot, M.R., 2003. Saharan dust storms and indirect aerosol effects on clouds: CRYSTAL-FACE results. Geophysical ResearchLetters 30 (12), 1633.

Schnitchen, C., Charman, D.J., Magyari, E., Braun, M., Grigorszky, I., Tóthmérész, B., Molnár, M. & Szántó, Zs., 2006. Reconstructing hydrological variability from testate amoebae analysis in Carpathian peatlands. Journal of Paleolimnology, 36, 1–17.

Shao, Y. P. 2008. Physics and Modelling of Wind Erosion 2nd edn. (Heidelberg: Springer). pp. 119.

Sherratt, A. G. 1981. Plough and pastoralism: aspects of the Secondary Products Revolution. InPattern of the Past (eds I. Hodder, G. Isaac and N. Hammond). Cambridge: Cambridge UniversityPress, pp. 261–306

Shichang, K., Dahe, Q., Mayewski, P. A., Wake, C. P., & Jiawen, R., 2001. Climatic and environmental records from the far east Rongbuk ice core, Mt. Qomolangma (Mt. Everest). Episodes, 24(3), 176-181.

Shotyk, W., Krachler, M., Martinez-Cortizas, A., Cheburkin, A. K., & Emons, H., 2002. A peat bog record of natural, pre-anthropogenic enrichments of trace elements in

ACCEPTED MANUSCRIPT

atmospheric aerosols since 12 370 14C yr BP, and their variation with Holocene climate change. *Earth and Planetary Science Letters*, *199*(1-2), 21–37. http://doi.org/10.1016/S0012-821X(02)00553-8

Tanţău, I., Reille, M., de Beaulieu, J. L., & Fărcas, S. 2006. Late Glacial and Holocene vegetation history in the southern part of Transylvania (Romania): pollen analysis of two sequences from Avrig. Journal of Quaternary Science, 21(1), 49-61.

Tanţău, I., Feurdean, A., de Beaulieu, J. L., Reille, M., & Fărcaş, S. 2011. Holocene vegetation history in the upper forest belt of the Eastern Romanian Carpathians. Palaeogeography, Palaeoclimatology, Palaeoecology, 309(3), 281-290.

Tanţău, I., Feurdean, A., de Beaulieu, J. L., Reille, M., & Fărcaş, S. 2014a. Vegetation sensitivity to climate changes and human impact in the Harghita Mountains (Eastern Romanian Carpathians) over the past 15 000 years. Journal of Quaternary Science, 29(2), 141-152.

Tanţău, I., Geantă, A., Feurdean, A., Tămaş, T., 2014b. Pollen analysis from a high altitude site in Rodna Mountains (Romania). Carpathian Journal of Earth and Environmental Sciences 9(2), 23-30.

Tămaş, T., Ferenc, K. and Barbu-Tudoran, L. 2011. Mineralogy of Iza Cave (Rodnei Mountains, N Romania). International Journal of Speleology 40: 171–179.

Tegen, I., Fung, I., 1995. Contribution to the atmospheric mineral aerosol load from land surface modification. J. Geophys. Res. 100, 18707–18726.

Tegen, I., Werner, M., Harrison, S. P., & Kohfeld, K. E., 2004. Relative importance of climate and land use in determining present and future global soil dust emission. Geophysical Research Letters, 31(5).

ACCEPTED MANUSCRIPT

Tudyka, K., Pazdur A., De Vleeschouwer F., Lityńska-Zając M., Chróst L. and Fagel N. 2017. Holocene elemental, lead isotope and charcoal record from peat in southern Poland, Mires and Peat, 19, 1–18.

Varga, G., Cserháti, C., Kovács, J., & Szalai, Z. 2016. Saharan dust deposition in the Carpathian Basin and its possible effects on interglacial soil formation. Aeolian Research, 22, 1-12.

Verschuren, D. 2004. Decadal and century-scale climate variability in tropical Africa during the past 2000 years. In Past climate variability through Europe and Africa (pp. 139-158). Springer Netherlands.

Wanner, H., Solomina, O., Grosjean, M., Ritz, S. P., & Jetel, M. 2011. Structure and origin of Holocene cold events. Quaternary Science Reviews, 30(21), 3109-3123.

Wentworth, C. K., 1922. A scale of grade and class terms for clastic sediments. The Journal of Geology, 30(5), 377-392.

Woronko, B. and Bujak, Ł., 2018. Quaternary aeolian activity of Eastern Europe (a Poland case study). Quaternary International, 478, pp.75-96.

ACCEPTED MANUSCRIPT

Figure captions

Figure 1A. Location of the study area in Europe (1) and the sites used for comparison: 2. Hautes Fagnes - Begium (Allan et al. 2013), 3. Slowínskie Blota - Poland (De Vleeschouwer et al., 2009), 4. Etang de la Gruère - Switzerland (Le Roux et al., 2012), 5. Mohos (Longman et al., 2017), 6. Hasvik - Norway (Sjögren, 2009), 7. Store Mosse bog – Sweden (De Jong et al., 2007), 8. Undarsmosse bog - Sweden (De Jong et al., 2007), 9. Hyltemossen bog - Sweden (Björck and Clemmensen, 2004). Blue arrows represent winter and red arrows summer wind directions (Anthoni, 2000). Figure 1B. Geological setting of the studied zone (after Kräutner et al., 1982).

Figure 2. Age-depth model from Tăul Muced peat bog.

Figure 3. Concentration of each grain size grouped into 3 size classes as derived from manual counting, total concentration of grains in a cm^3, aeolian sand influx, maximum grain size and the mineralogical composition (quartz - black, blue - calcite, others - red). The yellow zones represent periods with enhanced erosion, transport and deposition of sand.

Figure 4. Grain size determined by laser-based particle size analysis. Size classes defined using Udden-Wentworth grain-size classification scheme (Wentworth, 1922).

Figure 5. Physical and geochemical properties of the peat core from Tăul Muced. The maximum grain size is derived from the manual counting of particles, while the median grain size is derived through laser-based particle size analysis (PHI–primary human indicators, SHI–secondary human indicators; CHAR–macro-charcoal accumulation rate).

ACCEPTED MANUSCRIPT

Figure 6. Calculated dust and sand influx. The red line represents the lowest smoothing of the represented parameters.

Figure 7. Comparing Tăul Muced results with published dust flux studies across Europe. The black bars across the base represent the cold events described by Wanner et al. (2011).

ACCEPTED MANUSCRIPT

Period	Age (cal yr BP)	Median quartz content (%)	Quartz standard deviation (%)	Minimum quartz content (%)	Mean calcite content (%)	Mean of others (%)
1	2086-present	89.40	14.95	20	4.75	5.83
2	3356-2086	87.11	12.89	47.61	7.87	5.05
3	5872-3356	97.39	3.45	88.88	1.74	0.85
4	7800-5872	93.37	5.95	80.95	5.00	1.62

Table 1. Relative mineralogical composition of sand particles during the four periods highlighted by cluster analysis (Q - quartz, Ca - calcite).

ACCEPTED MANUSCRIPT

	Size (μm)	100-200	200-300	300-400	400-500	500-600	600-700	700-800	800-900	>900
no. of particles/sample	Min	0	0	0	0	0	0	0	0	0
	Max	239	46	35	9	5	2	2	1	2
	Mean	30.07	5.48	1.62	0.55	0.19	0.09	0.05	0.01	0.04
	Stdev	39.71	7.10	3.19	1.16	0.61	0.333	0.25	0.11	0.22
	Avg. % of total	75.90%	16.26%	4.52%	2.06%	0.60%	0.34%	0.16%	0.05%	0.11%

Table 2. Statistical parameters for each class of manually counted grain sizes.

ACCEPTED MANUSCRIPT

Scale	**Clay**	**Very fine silt**	**Fine silt**	**Medium silt**	**Coarse silt**	**V. fine sand**	**Fine sand**	**Medium sand**	**Coarse sand**
Size (µm)	<3.9	3.9-7.8	7.8-15.6	15.6-31	31-63	63-125	125-250	250-500	500-1000
Min	0.00	1.17	14.80	15.38	0.39	0.00	0.00	0.00	0.00
Max	2.04	23.72	63.78	45.84	32.59	22.49	11.92	11.15	5.44
Mean	0.07	4.50	30.04	35.03	19.23	8.25	2.29	0.47	0.12
Stdev	0.19	2.65	9.39	5.53	7.39	5.58	2.25	1.08	0.62

Table 3. Statistical parameters for each of grain size class determined by laser-based particle size analysis.

ACCEPTED MANUSCRIPT

Period (cal yr BP)	Romania (this study)	Romania (Longman et al., 2017),	Poland (De Vleeschouwer et al., 2009)	Switzerland (Le Roux et al., 2012)	Belgium (Allan et al. 2013)
Last 200 years	High	-	High	High	-
LIA	Low	Low	High	High	-
MWP	High	Increase in the last part	Low	Low	-
2400-1600	Low	High	-	High	Low
3600-2400	High; peak at 3000-2800	A single increase, but generally low	-	High, peak at 3600-3200	High, peak at 2800-2600
4200-3800	High	Some increase	-	High	Slight increase about 4.2 ka
6200-4200	Low	Low	-	Low	Generally low with some peaks around 5000 BP
6400-6200 cold event	Yes	Slight increase	-	Yes	No
7800-6400	Low	Low	-	Low	Low

Table 4. Summary of the key trends in peat-based dust flux studies across Europe (red – higher dust fluxes, blue – low dust fluxes).

Highlights:

- Reconstruction of past aeolian fluxes using ombrotrophic mountain bog
- Four major shifts in aeolian fluxes in the past 7800 years.
- Identify the relationship between aeolian fluxes and their controlling factors.
- Aeolian fluxes were primarily influenced by climate and anthropogenic drivers
- Comparison with other records of aeolian estimates from central and northwest Europe

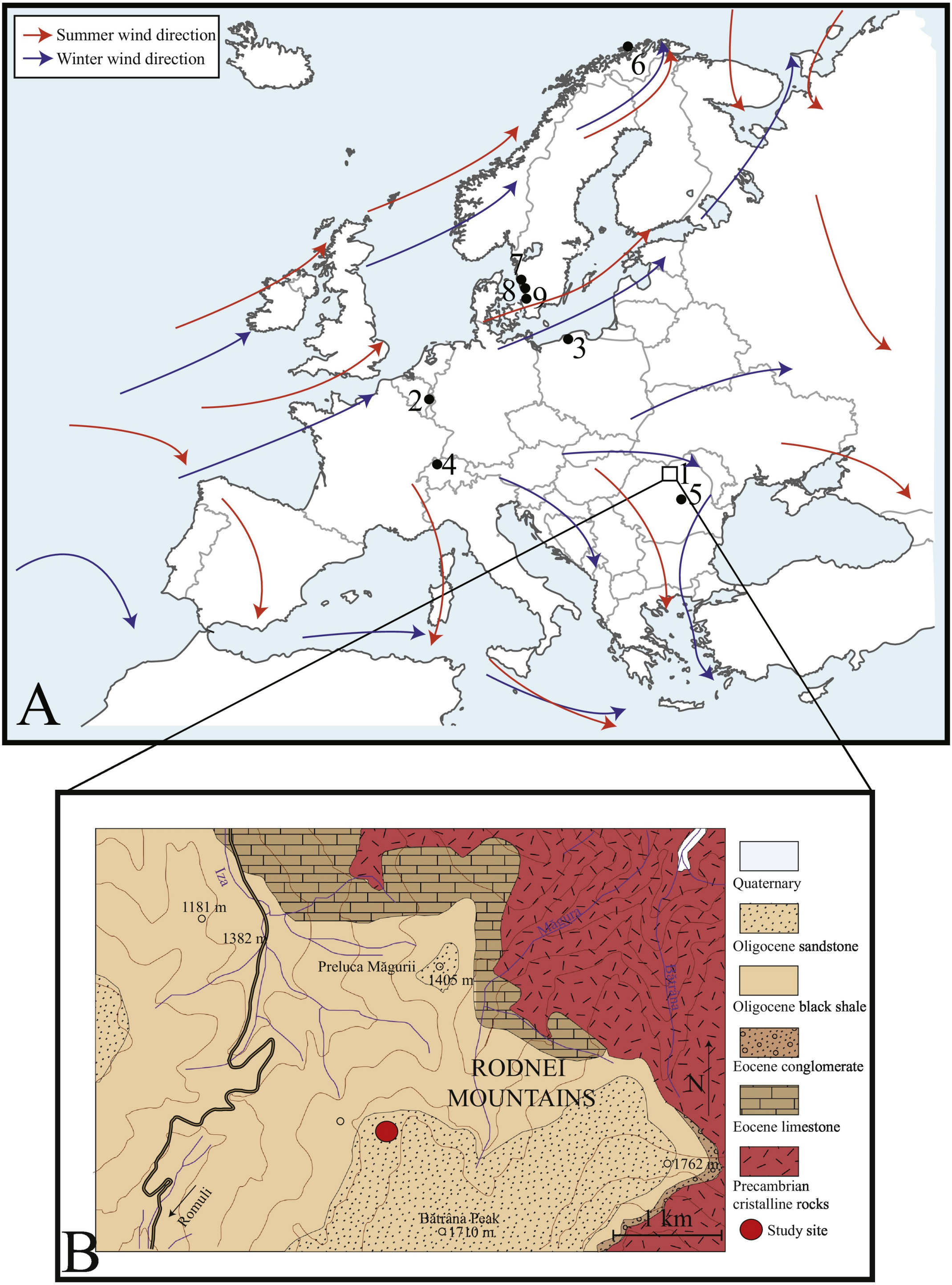

Summer wind direction
Winter wind direction
1
2
3
4
5
6
7
8
9
A
Quaternary
Oligocene sandstone
Oligocene black shale
Eocene conglomerate
Eocene limestone
Precambrian cristalline rocks
Study site
Iza
1181 m
1382 m
Preluca Măgurii
1405 m
Măgura
Bătrâna
RODNEI MOUNTAINS
N
1762 m
Romuli
Bătrâna Peak
1710 m
1 km
B

Figure 1

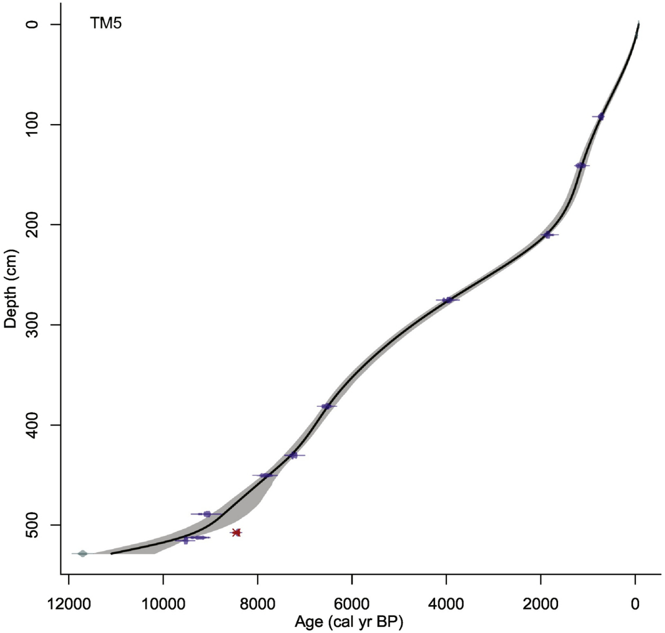
TM5
Depth (cm)
0
100
200
300
400
500
12000
10000
8000
6000
4000
2000
0
Age (cal yr BP)

Figure 2

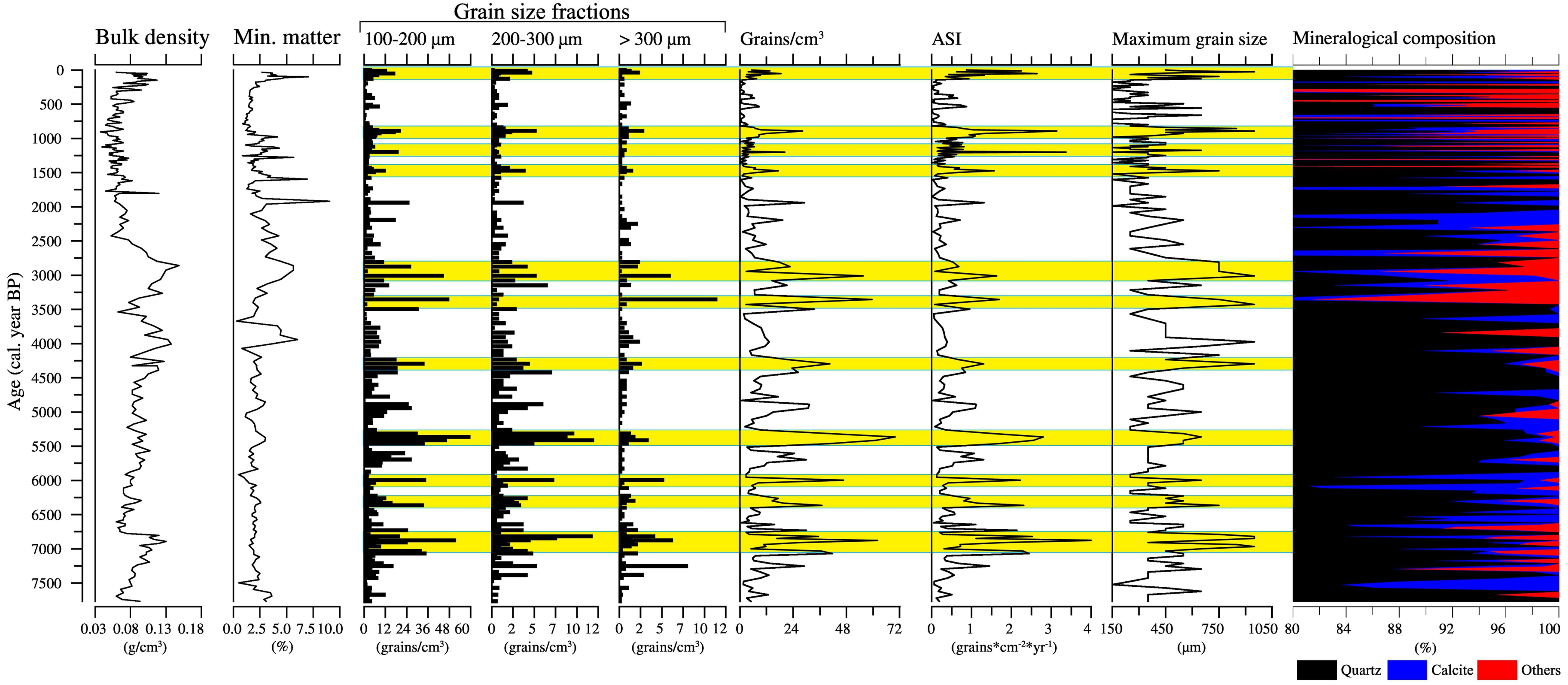
Grain size fractions
Bulk density
Min. matter
100-200 µm
200-300 µm
> 300 µm
Grains/cm³
ASI
Maximum grain size
Mineralogical composition
Age (cal. year BP)
0
500
1000
1500
2000
2500
3000
3500
4000
4500
5000
5500
6000
6500
7000
7500
0.03 0.08 0.13 0.18
(g/cm³)
0.0 2.5 5.0 7.5 10.0
(%)
0 12 24 36 48 60
(grains/cm³)
0 2 5 7 10 12
(grains/cm³)
0 2 5 7 10 12
(grains/cm³)
0 24 48 72
0 1 2 3 4
(grains*cm-2*yr-1)
150 450 750 1050
(µm)
80 84 88 92 96 100
(%)
Quartz
Calcite
Others

Figure 3

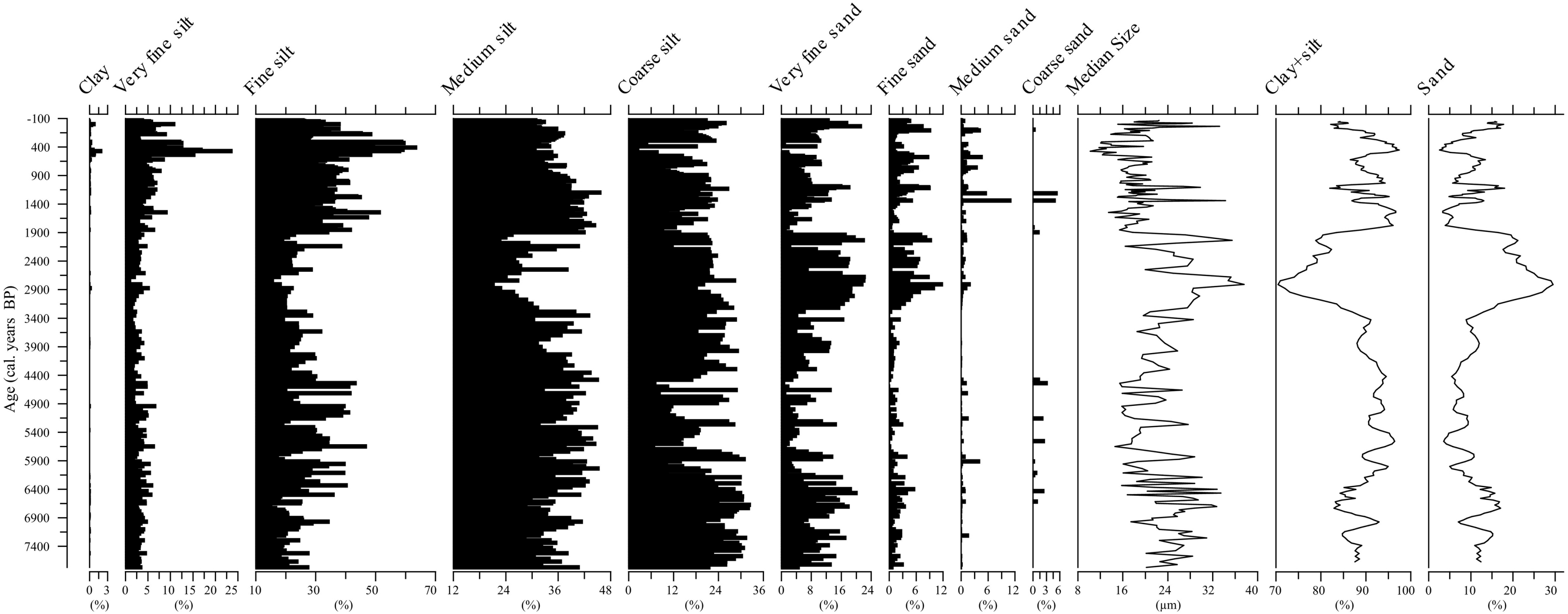

Clay
Very fine silt
Fine silt
Medium silt
Coarse silt
Very fine sand
Fine sand
Medium sand
Coarse sand
Median Size
Clay+silt
Sand
Age (cal. years BP)
-100
400
900
1400
1900
2400
2900
3400
3900
4400
4900
5400
5900
6400
6900
7400
(%)
(μm)

Figure 4

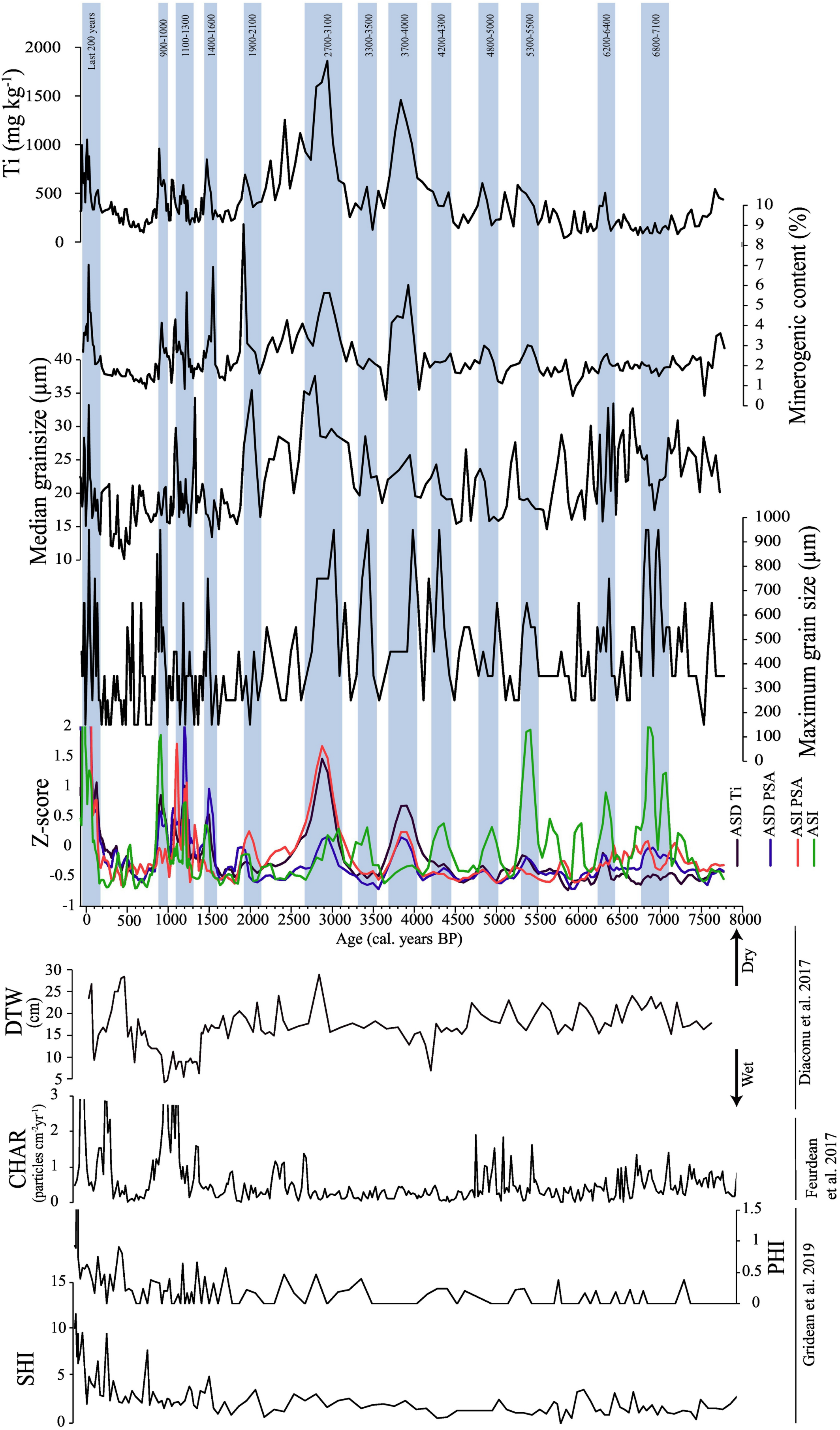
Last 200 years
900-1000
1100-1300
1400-1600
1900-2100
2700-3100
3300-3500
3700-4000
4200-4300
4800-5000
5300-5500
6200-6400
6800-7100
Ti (mg kg-1)
Minerogenic content (%)
Median grainsize (µm)
Maximum grain size (µm)
Z-score
ASD Ti
ASD PSA
ASI PSA
ASI
Age (cal. years BP)
Dry
Wet
DTW (cm)
Diaconu et al. 2017
CHAR (particles cm-2yr-1)
Feurdean et al. 2017
PHI
Gridean et al. 2019
SHI

Figure 5

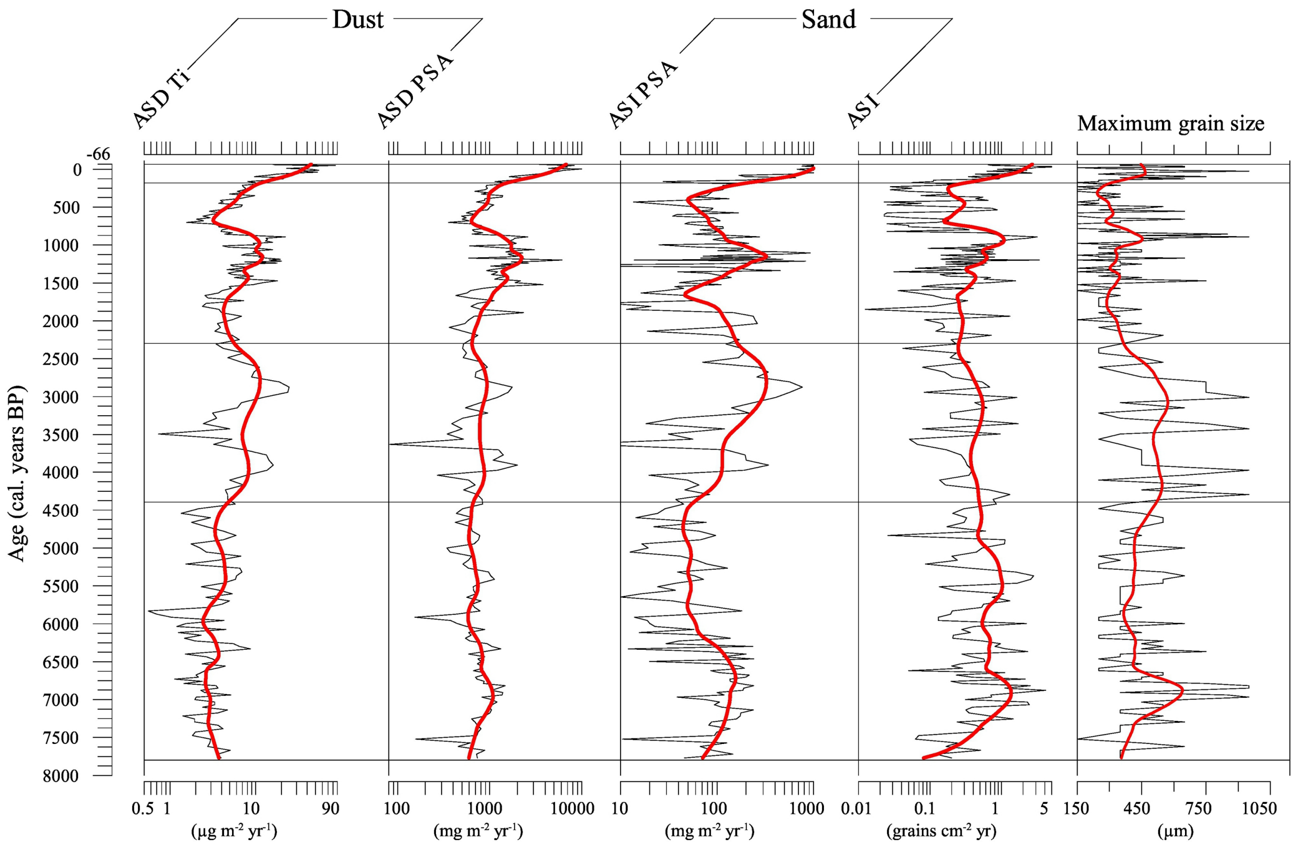

Dust
Sand
ASD Ti
ASD PSA
ASI PSA
ASI
Maximum grain size
-66
Age (cal. years BP)
0.5 1 10 90
(µg m-2 yr-1)
100 1000 10000
(mg m-2 yr-1)
10 100 1000
(mg m-2 yr-1)
0.01 0.1 1 5
(grains cm-2 yr)
150 450 750 1050
(µm)

Figure 6

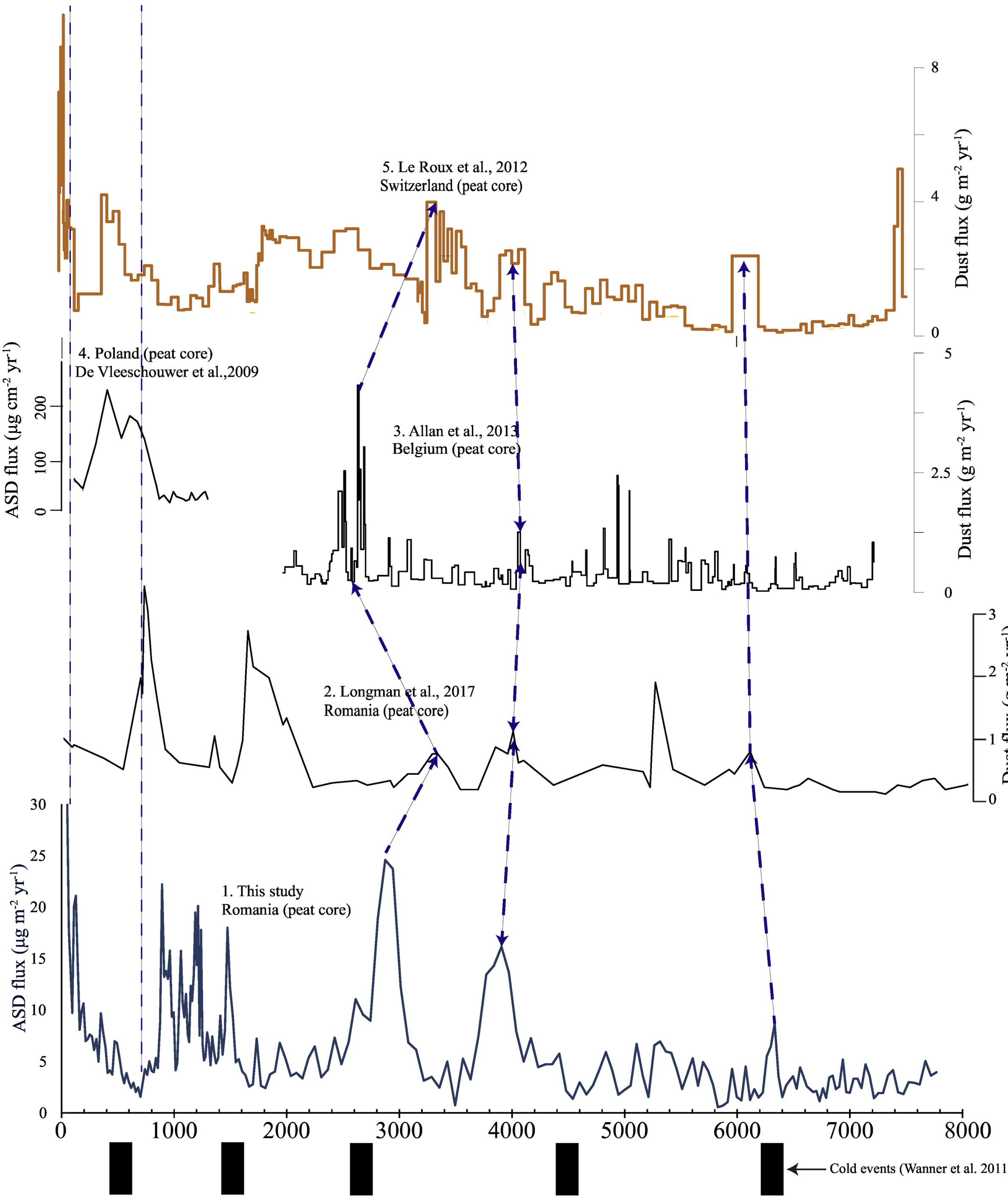
5. Le Roux et al., 2012
Switzerland (peat core)
Dust flux (g m^{-2} yr^{-1})
8
4
0
4. Poland (peat core)
De Vleeschouwer et al.,2009
ASD flux (µg cm^{-2} yr^{-1})
200
100
0
3. Allan et al., 2013
Belgium (peat core)
Dust flux (g m^{-2} yr^{-1})
5
2.5
0
2. Longman et al., 2017
Romania (peat core)
Dust flux (g m^{-2} yr^{-1})
3
2
1
0
1. This study
Romania (peat core)
ASD flux (µg m^{-2} yr^{-1})
30
25
20
15
10
5
0
0
1000
2000
3000
4000
5000
6000
7000
8000
Cold events (Wanner et al. 2011)

Figure 7